VILNIUS UNIVERSITY
CENTER FOR PHYSICAL SCIENCES AND TECHNOLOGY
SEMICONDUCTOR PHYSICS INSTITUTE

PAULIUS RAGULIS

DEVELOPMENT, RESEARCH AND APPLICATION OF WIDE BAND RESISTIVE SENSORS

Summary of doctoral thesis

Physical sciences, physics (02 P), semiconductor physics (P 265)

Vilnius 2013

The research has been carried out in 2008 – 2013 at the Microwave laboratory of Semiconductor Physics Institute, Center for Physical Sciences and Technology

Scientific supervisor:

Habil. dr. Žilvinas Kancleris (CPST Semiconductors physics institute, Physical sciences, physics – 02P, semiconductor physics – P265)

Consultant:

Prof. dr. Vincas Tamošiūnas (Vilnius University, Physical sciences, physics – 02P, semiconductor physics – P265)

Council of defence of the doctoral thesis of Physical Sciences at Vilnius University:

Chairman:

Prof. dr. Vidmantas Remeikis (CPST Institute of physics, Physical sciences, physics – 02P, Nuclear physics – P220)

Members:

Prof. dr. Algirdas Baškys (Vilnius Gediminas technical university, Technological sciences, electrical and electronics engineering – 01T, electronics – T170)

Prof. habil. dr. Antanas Čenys (Vilnius Gediminas technical university, Physical sciences, physics – 02P, semiconductor physics – P265)

Prof. habil. dr. Antanas Feliksas Orliukas (Vilnius University, Physical sciences, physics – 02P, semiconductor physics – P265)

Doc. dr. Arūnas Šetkus (CPST Semiconductors physics institute, Physical sciences, physics – 02P, semiconductor physics – P265)

Opponents:

Prof. dr. Vytautas Urbanavičius (Vilnius Gediminas technical university, Technological sciences, electrical and electronics engineering – 01T, high frequency technology, microwaves – T191)

Dr. Irmantas Kašalynas (CPST Semiconductors physics institute, Physical sciences, physics – 02P, semiconductor physics – P265)

The official defence of doctoral thesis will be held in public session of Vilnius university Defence Council of Physical sciences at 14 h. on September 20, 2013 in the Conference hall of the Semiconductor Physics Institute (Center for Physical Sciences and Technology), A. Goštauto 11, LT – 01108 Vilnius, Lithuania.

The summary of the doctoral thesis has been distributed on August 20, 2013.

The doctoral thesis is available at the libraries of Vilnius University and Center for Physical Sciences and Technology.

VILNIAUS UNIVERSITETAS
FIZINIŲ IR TECHNOLOGIJOS MOKSLŲ CENTRAS
PUSLAIDININKIŲ FIZIKOS INSTITUTAS

PAULIUS RAGULIS

PLAČIAJUOSČIŲ MIKROBANGŲ JUTIKLIŲ KŪRIMAS, TYRIMAS IR TAIKYMAS

Daktaro disertacijos santrauka

Fiziniai mokslai, fizika (02 P), puslaidininkių fizika (P 265)

Vilnius 2013

Disertacija rengta 2008 – 2013 metais FTMC Puslaidininkių fizikos instituto Mikrobangų laboratorijoje

Mokslinis vadovas:

Habil. dr. Žilvinas Kancleris (FTMC Puslaidininkių fizikos institutas, fiziniai mokslai, fizika – 02P, puslaidininkių fizika – P265)

Konsultantas:

Prof. dr. Vincas Tamošiūnas (Vilniaus universitetas, fiziniai mokslai, fizika – 02P, puslaidininkių fizika – P265)

Disertacija ginama Vilniaus Universiteto Fizikos mokslų krypties taryboje:

Pirmininkas:

Prof. dr. Vidmantas Remeikis (FTMC Fizikos institutas, fiziniai mokslai, fizika – 02P, branduolinė fizika – P220)

Nariai:

Prof. dr. Algirdas Baškys (Vilniaus Gedimino technikos universitetas, technologiniai mokslai, elektros ir elektronikos inžinerija – 01T, elektronika – T170)

Prof. habil. dr. Antanas Čenys (Vilniaus Gedimino technikos universitetas, fiziniai mokslai, fizika – 02P, puslaidininkių fizika – P265)

Prof. habil. dr. Antanas Feliksas Orliukas (Vilniaus universitetas, fiziniai mokslai, fizika – 02P, puslaidininkių fizika – P265)

Doc. dr. Arūnas Šetkus (FTMC Puslaidininkių fizikos institutas, fiziniai mokslai, fizika – 02P, puslaidininkių fizika – P265)

Oponentai:

Prof. dr. Vytautas Urbanavičius (Vilniaus Gedimino technikos universitetas, technologiniai mokslai, elektros ir elektronikos inžinerija – 01T, Aukštų dažnių technologijos, mikrobangos – T191)

Dr. Irmantas Kašalynas (FTMC Puslaidininkių fizikos institutas, fiziniai mokslai, fizika – 02P, puslaidininkių fizika – P265)

Disertacija bus ginama viešame Fizikos mokslo krypties tarybos posėdyje 2013 m. rugsėjo mėn. 20 d. 14 valandą Fizinių ir technologijos mokslų centro Puslaidininkių fizikos instituto posėdžių salėje A. Goštauto 11, LT-01108, Vilnius, Lietuva.

Disertacijos santrauka išsiuntinėta 2013 m. rugpjūčio mėn. 20 d.

Disertaciją galima peržiūrėti Vilniaus universiteto bei Fizinių ir technologijos mokslų centro bibliotekose

Santrauka

Pagrindinis darbo tikslas – sukurti plačiajuostį rezistorinį jutiklį, skirtą didelės galios mikrobangų impulsams matuoti, kurio jautrusis elementas pagamintas iš n-tipo Si yra įmontuotas H tipo bangolaidyje. Rezistorinis jutiklis turėtų pasižymėti plokščia jautrio dažnine charakteristika, jo varža neviršyti 1 kΩ, o stovinčios bangos koeficientas būti mažesnis nei 1,5.

Disertacijoje yra pateikiami teoriniai elektrinio lauko pasiskirstymo bangolaidinėje sekcijoje su rezistorinio jutiklio jautriuoju elementu viduje modeliavimo baigtinių skirtumų laiko skalėje metodu rezultatai, kai jautrusis elementas yra talpinamas standartiniuose H tipo bangolaidžiuose WRD250 ir WRD840. Modeliavimo metu buvo ieškoma tokių jautriojo elemento matmenų ir savitosios varžos, kad rezistorinis jutiklis tenkintų aukščiau paminėtus reikalavimus. Disertacijoje taip pat aprašomi trijų skirtingų rezistorinių jutiklių, kurių optimalūs matmenys buvo surasti iš modeliavimo rezultatų, eksperimentiniai tyrimai. Buvo nustatytos šių jutiklių jautrio dažninės charakteristikos, jutiklių atsako signalo priklausomybė nuo mikrobangų galios ir stovinčios bangos koeficientas. Sujungus sukurtąjį jutiklį su plačiajuoste ruporine antena buvo atlikti mikrobangų galios tankio (elektrinio lauko stiprio) matavimai atviroje erdvėje. Praktines rezistorinių jutiklių taikymo galimybes demonstruoja disertacijoje pateikti internetinių maršrutizatorių ir šviesolaidinių konverterių elektromagnetinio atsparumo tyrimai, kuriuose rezistoriniai jutikliai naudojami elektrinio lauko stipriui nustatyti.

List of abbreviations used in text

RS – resistive sensor

SE – sensing element

HPM – high power microwave

VSWR – voltage standing wave ratio

FDTD – finite-difference time-domain

Introduction

Nowadays growing and expanding modern communication networks occupy a significant part of our everyday life. Complex and integrated chips are used in the communication and automation systems. The amount of information transferred between networks increases rapidly and data can be transferred between many different systems such as computers, sensors, radars, etc. On the one hand, the miniaturization of electronic components used in communication networks makes these devices more vulnerable to high power microwave (HPM) radiation, which may result in the disturbance of their functionality or even disruption. On the other hand, the progress in the development of compact HPM generators results in the threat of deliberate electronic attacks in order to interfere or disrupt the functionality of critical civil or military communication networks. To evaluate the vulnerability of electronic systems their resistance against HPM pulses is tested. During such investigations the power of HPM pulses should be measured permanently. The large number of measurements involved and their importance dictate that the measurement equipment and techniques should be accurate, reproducible, and convenient to use.

One of the perspective devices for the measurement of HPM pulse power is a resistive sensor (RS) [1], performance of which is based on a hot electron phenomenon in semiconductors. The RS demonstrates some advantages when it is used for HPM pulse measurement. It measures HPM pulses directly, produces high output signal, and exhibits excellent long term stability [1]. Since the RS is devoted to HPM pulse measurement, the rectangular waveguide layout is usually used for its implementation. The main disadvantage of these sensors is a narrow frequency band limited by the pass-band of the rectangular waveguide. It is possible to widen this frequency more than two times by employing a double ridge waveguide for the RS implementation. Connecting the developed RS to a wide band horn antenna, electric field strength measurement in free space can be performed, broadening application of the sensors in electromagnetic susceptibility experiments.

In this thesis, the results of the theoretical calculation of electromagnetic fields inside a sensing element (SE) of the RS implemented in WR90, WRD250 and WRD840

waveguides are presented. Using the values of the average electric field in the SE the dependence of sensitivity on frequency is calculated, allowing the engineering of the RS with a desirable frequency response. The experimental investigation results of the RS implemented in WR90 and WRD250 waveguides are presented. It is demonstrated that by combining the dependence of antenna gain on frequency and parameters of resistive sensors it is possible to create the system made of the resistive sensor and the horn antenna, with flat frequency response. The investigations of the electromagnetic susceptibility of internet routers and media converters were also performed using the resistive sensors to measure electric field strength near the device under test.

The main goal of the thesis was to create the resistive sensor implemented in a double-ridged waveguide with flat frequency response. The resistance of the sensor should be lower than 1 kΩ and voltage standing wave ratio (VSWR) lower than 1.5. The characteristics of these sensors were investigated experimentally. By connecting the resistive sensor to the wide band horn antenna microwave pulse power density (electric field strength) measurements in free space were performed.

Main objectives:

- To calculate electromagnetic field components in a sensing element of the RS implemented in WR90, WRD250 and WRD840 waveguides by using finite – difference time – domain method finding optimal electro physical parameters: dimensions and resistivity of the SE.
- To investigate experimentally the characteristics of the manufactured resistive sensors with found optimal parameters, also performing measurements of the microwave pulse power density (electric field strength) in free space.
- To demonstrate the practical use of the resistive sensors in the investigations of the electromagnetic susceptibility of the electronic devices.

Statements to defend:

- Normalized electric field inside the sensing element of the resistive sensor, mounted in the double ridge waveguide, depends on its transverse dimensions and resistivity. Therefore, by changing these parameters the decrease of the electric field in the sensing element with frequency, occurring due to the wave dispersion in the waveguide, can be compensated.
- The wideband resistive sensor, the sensing element of which is made from 10 Ω·cm resistivity n-Si with dimension $h \times w \times l = 3.8 \times 1 \times 1$ mm^3, measures high power microwave pulses in 2.6 – 7.8 GHz frequency band (WRD250 waveguide). The variation of the sensitivity of the sensor on frequency is ±25% within pass band of the waveguide.
- Considering the dependence of gain of the horn antenna on frequency and choosing suitable parameters of the resistive sensor the measurement system, made of the horn antenna and resistive sensor, can be composed for electric field measurements in free space with flat frequency response.
- 1 Gb/s speed internet routers are the most vulnerable to the higher frequency (5.7 GHz) microwave radiation while 100 Mb/s speed internet routers are the most susceptible to the lower frequency 2.75 GHz microwave pulses.

Contribution of the author

The author of the thesis performed theoretical simulations of the resistive sensors implemented in the double ridge waveguide and chose the optimal set of the SE parameters. He manufactured sensing elements and assembled them in the waveguide. The author performed experimental investigations of the sensors and demonstrated the application of the resistive sensors in electromagnetic susceptibility experiments. The significant input of the author to the preparation of the scientific papers and conference contributions related to the thesis should be acknowledged.

Layout of the thesis

The thesis consists of the introduction, five chapters, conclusions and a list of references. Short summaries of each chapter are presented below.

1 Introduction

In the introductory chapter of the thesis the relevance of the work is justified, main goal and objectives of the thesis are formulated. Readers are introduced to the statements to be defended. The scientific articles and conference contributions of the author related to the thesis are listed.

2 Review of scientific articles related to thesis

The second chapter describes the state of the art in a field related to the investigations performed in the thesis. The chapter consists of five sections. In the first section the review on microwave power measurement placing special emphasis on the methods applicable in the HPM field is presented. In the second section the information about double ridged waveguide is given. The types of electromagnetic interference and models describing the susceptibility of the devices are reviewed in the third section. In the next section a finite-difference time-domain method (FDTD) used for the calculation of electromagnetic field components is briefly described. In the last section of the chapter short summary of the review is presented.

2.1 Microwave measurements

Devices used for microwave power measurement, their principle of operation, advantages and disadvantages are reviewed in this section with more attention given to newest scientific results and possible application of these devices to measure HPM pulses. This section is divided into two subsections.

Principles of the operation and the newest scientific results of the thermistors and thermocouples are presented in the first subsection. Almost few decades they are the most popular sensors to measure average microwave power. These devices are commonly used both in the industry and scientific laboratories.

The average power meters can be used for the microwave pulse power measurement as well. The pulse power measurement is straightforward, when microwave pulses are rectangular and their repetition rate is high. However, it is impossible to use such type of sensors to measure pulse power when the microwave pulse shape is not rectangular. It is also difficult to perform the measurements of low repetition rate or single pulses. In order to measure such microwave signals, pulsed power sensors has to be employed. So in the second subsection three different types of pulsed power microwave sensors are reviewed: microwave diodes, electro optic and resistive sensors.

2.2 Double ridge waveguide

For the first time a double ridged waveguide was mentioned in the work of S. B. Cohn [2] in 1947. Later on more detailed analysis of these waveguides was published in 1955 by S. Hopfer [3]. The double ridge waveguide has two ridges inserted along the wide walls of the waveguide. The region between the ridges is usually named as a gap. The cross-sectional view of the double ridge waveguide shown in Fig. 1 is suggestive of a letter H, so sometimes it is named as an H-type waveguide. The ratio between the highest and the lowest passing frequencies for a double ridge waveguide in a number of series is $f_{MAX}/f_{MIN} \approx 3$, whereas for a traditional rectangular waveguide this ratio is 1.5. From this point of view the double ridged waveguide is very attractive, since its pass band is more than two times wider than the rectangular one. Therefore by implementing the RS in the double ridge waveguide, the extension of the frequency band of the resistive sensor can be accomplished.

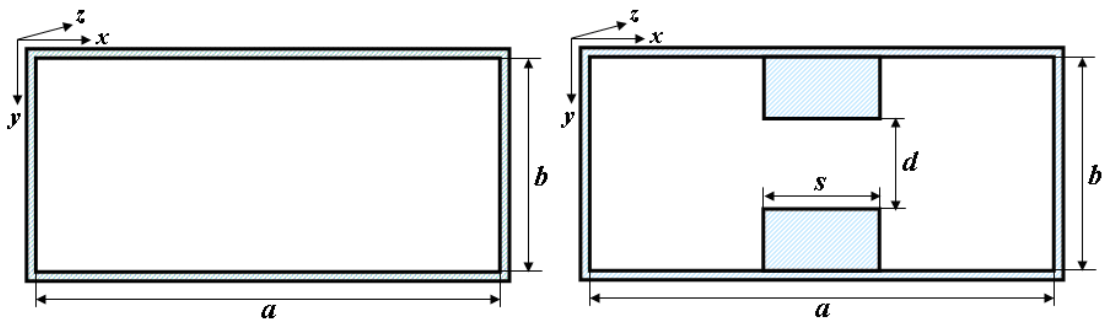

Fig. 1 Rectangular (left) and double ridge (right) waveguides.

2.3 Electromagnetic susceptibility

The failures occurring in electronic devices subjected to HPM pulses generally can be divided into disruptive and regenerative. The disruptive failure means that the electronic device or a part of it is physically damaged and to fix it the device or some part of it should be replaced. The regenerative failure means that the device under radiation losses its functionality but it can be restored when the radiation is switched off. The regenerative failures, in turn, can be divided into two groups. At a lower radiation level the loss of the functionality of the device is self recovering: it gets back when the radiation is turned off. At a higher radiation level the device is unable to recover without operator intervention therefore the restart or the hard reset should be done.

In general, the failure phenomenon of electronic devices, affected by the electromagnetic radiation, has been considered using two basic approaches: thermal heating and parasitic charging.

A thermal heating model considers the overheating of the specific regions of the electronic device by external microwave pulse over some critical temperature, which causes the failure of the device. Depending on the pulse length three main regions of the heating process can be distinguished: adiabatic, quasi-static and intermediate one [4].

A parasitic charging model describes the accumulation of a parasitic charge as a result of microwave rectification on a nonlinear element of the electronic device. The microwave pulse charges the capacitor, which in turn results in the failure of the device.

2.4 Finite-difference time-domain method

We used a FDTD method for the calculation of the electromagnetic field components in the RS [5]. Using this method all the volume of interest is filled with points where the components of electric and magnetic field are calculated. The points in the volume are shifted with respect to each other by a half of a step. Therefore, each component is actually calculated in a different place. Time and coordinate derivatives in the Maxwell equations are replace by finite differences and simple formulas are obtained to calculate the new values of the electromagnetic field components from the older ones. In a time domain, the calculations are performed at each half time step. Using the old values of the H components the new E components are determined and from them in the

next step the newest H components are found out. Such calculation scheme provides h^2 accuracy in both space and time domains. The details of the application of the FDTD technique can be found in [5].

3 Results of theoretical calculation

In this chapter the results of the theoretical calculation of electromagnetic fields inside waveguide segment with the SE of the resistive sensor implemented in the waveguide are presented. Calculations have been performed using FDTD method. From the modelling results the dimensions and the specific resistance of the sensing element were chosen for the sensor that meets the following requirements: its resistance should be lower than 1 kΩ and voltage standing wave ratio lower than 1.5, and the frequency response of the sensor should be as flat as possible. The chapter is divided into two parts. In the first part the results for the resistive sensor with the sensing element mounted inside the WR90 (8.2 – 12.4 GHz) waveguide are presented. The second part is dedicated to the resistive sensor implemented in WRD250 (2.6 – 7.8 GHz) and WRD840 (0.84 – 2.0 GHz) double ridged waveguides.

3.1 Resistive sensor implemented in WR90 waveguide

The first calculations were performed for the resistive sensor implemented in the standard WR90 waveguide (Fig. 2). Chosen configuration of the SE differs from the earlier employed layouts in this frequency band, namely, cross waveguide type RS [1], or diaphragm type RS [7]. As it is seen from Fig. 2, two sensing elements were used. The SE is made of n-type Si with ohmic contacts on the both ends. The lower contacts of the sensing elements are shorted with a thin metal foil. One of the upper contacts is

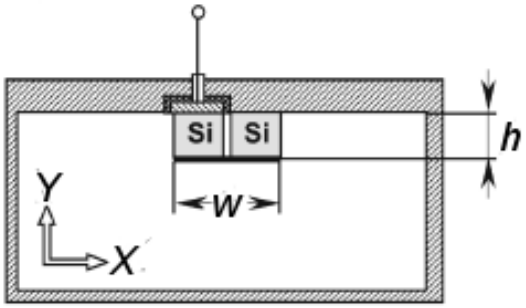

Fig. 2 Resistive sensor with two sensing elements implemented in WR90 waveguide. Sensing elements are made of n-type Si connected together with thin metal foil [6].

grounded whereas the other one is isolated from the waveguide. It is connected to the current source and the DC pulse measuring unit.

Sensitivity of the resistive sensor can be written as:

$$\zeta = \frac{3\beta E_0^2}{2P_\infty} \times \frac{1}{\sqrt{1-(\lambda/\lambda_c)^2}} \times \frac{\langle E \rangle^2}{E_0^2}, \quad (1)$$

where β is a warm electron coefficient defining the deviation of the current–voltage characteristic from Ohm's law in a DC electric field, P_∞ is a microwave power transmitted through the waveguide in a high frequency limit, $\langle E \rangle$ is an average of the electric field amplitude in the SE, E_0 is electric field strength in the centre of the empty waveguide, λ and λ_c are the wavelength of electromagnetic wave in free space and critical wavelength in the waveguide, respectively.

In (1) three multipliers can be distinguished. The first one is independent of the microwave frequency, since in the frequency range, considered in the thesis, electron heating inertia does not manifest itself and as a consequence the warm electron coefficient is independent of frequency [1]. The second multiplier in the expression accounts for the fact that due to the wave dispersion in the waveguide even at the same power level transmitted through the waveguide, the electric field strength in it decreases with frequency leading to the decrease of the sensitivity. The third multiplier is a square of the average of the electric field in the SE normalized to the amplitude of the electric field in the centre of the empty ridged waveguide that is calculated using the FDTD method.

As one can see from the expression (1), in order to get the sensitivity of the RS independent of frequency, the parameters of the SE have to be chosen in such a way that the average electric field amplitude in the SE should increase with frequency, compensating the decrease of the sensitivity due to the wave dispersion in the waveguide. A desirable dependence of the average electric field on frequency in the "ideal" SE can be calculated from (1). Further the term "ideal sensor" refers to the resistive sensor, the sensitivity of which is independent of frequency.

Theoretical calculations were started from the ρ = 30 Ω·cm resistivity sensing element. The width of the SE was set to w = 1.5 mm and the height was chosen h = 1 mm to fulfil the requirement of small reflection of the electromagnetic wave from

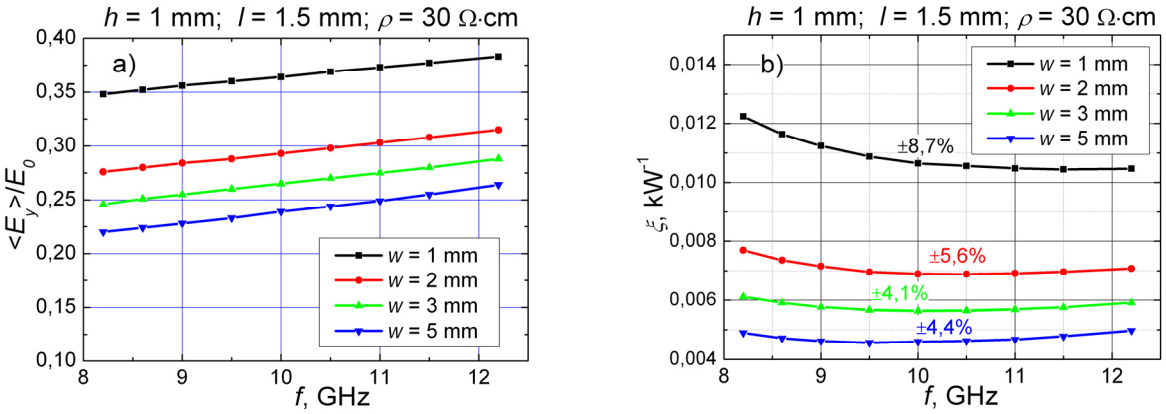

Fig. 3 Calculated electric field inside resistive sensors sensing element (a) and sensitivity's dependence on microwave frequency (b), when sensing element is mounted into WR90 waveguide.

the sensing elements. It was found that the optimal length of the SE is 1.5 mm. The second set of the calculations was performed to find the optimal width of the SE. It is seen from the Fig. 3a, that by widening the SE the average electric field inside the sensing element decreases. This decrease cannot be explained neither by the increased electromagnetic wave reflection from the SE nor by the distribution of the electric field in TE_{10} mode in the waveguide. It seems that the decrease of the total resistance of the SE has the largest influence to the decrease of $\langle E \rangle$. The sensing element can be considered as an external load. The resistance of it decreases when the transverse dimensions of the SE are increased. This, in turn, leads to the decrease of the electric field strength in the SE due to increased losses in it.

Calculated dependences of the sensitivity of the RS on frequency are shown in the Fig. 3b. The smallest sensitivity variation ±4.1% was found for the sensing element made of $\rho = 30$ Ω·cm, dimensions of which were $h \times w \times l = 1 \times 3 \times 1.5$ mm^3. This set of the parameters was chosen for the practical realization and further experimental investigation.

3.2 Resistive sensor implemented in WRD waveguide

In this section the RS implemented in the double ridge waveguide is considered. In the first three subsections the modelling results of the RS on a basis of the waveguide WRD250 (frequency range 2.6 – 7.8 GHz) are described. In the next subsection WRD840 (0.84 – 2.0 GHz) waveguide is considered. In the last subsection the results of the modelling of the RS connected to the wide band horn antenna are presented.

3.2.1 Two SE on the ridge of waveguide

The modelled RS, as in previous section, was composed of the two sensing elements, the height of which is smaller than the distance d between the ridges. Considering the ratio between the length of the SE and the wavelength of electromagnetic wave λ_d in the SE mounted in the waveguide, the simulated sensors were divided into two groups. In the first group the length of the SE is less than λ_d, while in the second group the length is comparable with λ_d. The simulations have revealed that for the first group of sensors the average electric field in the SE increases with frequency much more than it is necessary for the frequency response compensation. More suitable results have been obtained for the second group of the sensors. Namely, for the SE made of the 5 Ω·cm resistivity n-Si, dimensions of which are $h \times w \times l = 1 \times 2 \times 16$ mm^3, calculated sensitivity variation is $\zeta = 2.65 \times 10^{-4}$ kW^{-1} ± 20.4% in the frequency range 2.6 – 7.8 GHz. Although electro physical parameters of the SE providing a sufficiently flat frequency response have been found, the calculated sensitivity of the RS is very low. Having in mind that due to a smaller distance between the metal surfaces in the gap region the maximum pulse power transmitted through the double ridged waveguide is lower, the practical worth of such a RS is doubtful.

3.2.2 Cross waveguide type resistive sensor

Simulation results of the cross waveguide type RS shown in Fig. 4 is presented in this section. As it is seen from the figure the SE is inserted in the centre of the double ridged waveguide and covers the gap region. Its height h corresponds to d, the width is denoted as w and the length in a wave propagation direction is indicated as l. There are ohmic contacts on both sides of the SE. One of the contacts is grounded while the other one is isolated from the waveguide and connected to the current source and measuring unit.

Simulation results for different length l of the SE ($\rho = 10$ Ω·cm, $w = 1$ mm) are shown in Fig. 5. As one can see from Fig. 5a, the increase of the relative electric field with frequency is too small to get a flat frequency response for a short sample ($l = 1$ mm). However, by increasing l, the relative electric field dependence on frequency

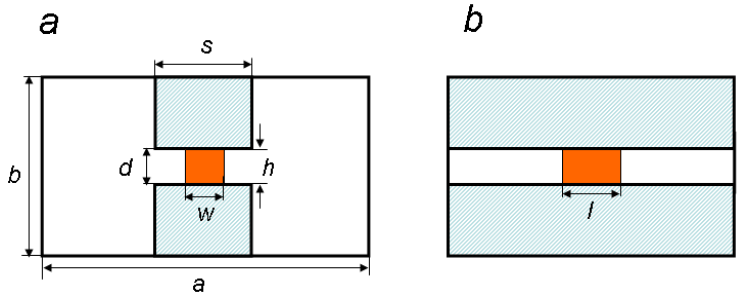

Fig. 4 Cross waveguide type resistive sensor: (a) front view, (b) side view.

approaches to the dependence characteristic of the ideal sensor. As follows from Fig. 5b, the average electric field in the SE decreases when the length l is growing, whereas the shape of the curve does not change much. This, in turn, leads to the observed increase of the relative electric field strength shown in Fig. 5a.

From the variety of dimensions and specific resistances of the investigated samples we chose a low (ρ = 10 Ω·cm) and high (ρ = 50 Ω·cm) specific resistance SE, the width of which is 1 mm. Calculation results for such sensors having different lengths l are shown in Fig. 6.

From the calculation results of the lower specific resistance (ρ = 10 Ω·cm) SE shown in Fig. 6a it is seen, that by increasing l the absolute value of sensitivity decreases. The smallest calculated sensitivity variation (±2.8%) was found at the l = 4 mm. Having in mind a wide frequency range of the WRD250 waveguide it should be an excellent result. Unfortunately, such a sensor is of little use due to a very large reflection. Its VSWR is roughly 2.5 and it is not acceptable for a measuring device. From the investigated samples, a sensor with cross-sectional dimensions $w \times l = 1 \times 1$ mm^2 can be considered as a prototype of the SE. Its sensitivity variation is ± 12.9%, VSRW < 1.4, and the DC resistance is 400 Ω.

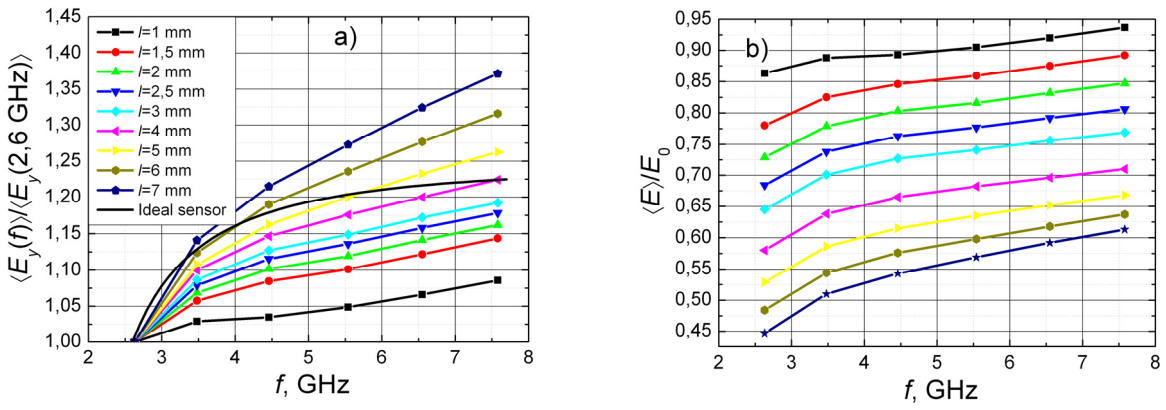

Fig. 5 Dependence of the relative electric field strength (a) and average electric field (b) in the sensing element on frequency for different length l of the SE: $h \times w = 4 \times 1$ mm^2, $\rho = 10$ Ω·cm, $\varepsilon = 11.9$.

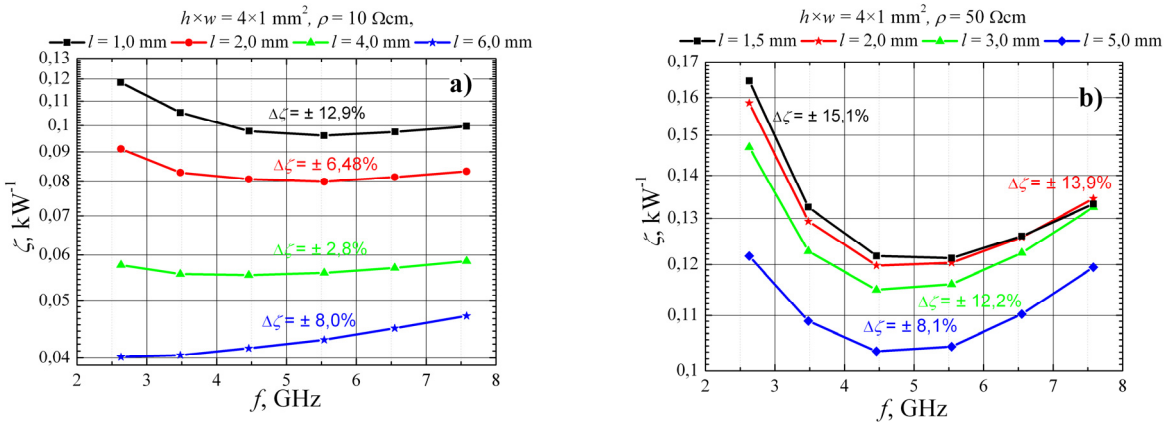

Fig. 6 Calculated sensitivity dependences on frequency for various length of the SE when $h \times w = 4 \times 1$ mm^2, $\varepsilon = 11.9$, $\rho = 10$ Ω·cm (a), $\rho = 50$ Ω·cm(b).

The results of calculations for ρ = 50 Ω·cm SE are shown in Fig. 6b. Taking into consideration the variation of sensitivity, reflection coefficient and DC resistance, it was found that the SE with cross-sectional dimensions $w \times l = 1 \times 3$ mm^2 is preferable. The calculated sensitivity variation is roughly ±12%, VSRW < 1.5, and the DC resistance is 670 Ω. As one can see from the Fig. 6b, the SE, the length of which is l = 5 mm, demonstrates even smaller sensitivity variation, namely ±8.1%. As in the case of the lower specific resistance SE, its reflection is too large and it cannot be used as a prototype of the RS.

For the further practical realization and experimental investigation two sensing elements were chosen: ρ = 10 Ω·cm with dimensions $w \times l = 1 \times 1$ mm^2 and ρ = 50 Ω·cm with dimensions $w \times l = 1 \times 3$ mm^2.

3.2.3 Resistive sensor with concentrator (WRD250)

Hoping to achieve the smaller sensitivity variation on frequency, the RS with concentrator shown in Fig. 7 was simulated. It is seen that the sensing element of such a resistive sensor occupies only a part of the waveguide window while the rest part is filled with a dielectric concentrator. As in the case of the WR90 waveguide, the RS is composed of the two sensing elements, which are separated from each other. On the one hand, the concentrator used in this layout leads to the increase of the electric field strength in the SE, comparing with the SE without concentrator described in the first subsection. On the other hand, the increase of the reflection from it should be taken into consideration.

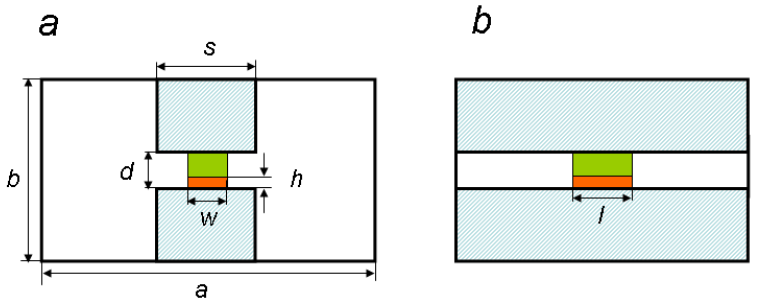

Fig. 7 Resistive sensor with concentrator: (a) front view, (b) side view.

The first simulations have been performed with three different dielectric constants of the concentrator: $\varepsilon_k = 2$, $\varepsilon_k = 5$, and $\varepsilon_k = 11.9$. It was found that by changing the dielectric constant of the concentrator there is no substantial influence to the dependence of the relative electric field on frequency. It means that the value of ε_k by itself has no significant influence on the frequency response of the RS. As it was expected, the increase of ε_k leads to the increase of the sensitivity of the RS.

As it is seen from the Fig. 8, the sensitivity of the sensor with concentrator also depends on the resistivity of the SE. So, by changing the resistivity of the SE, it becomes possible to achieve the smallest sensitivity variation on frequency. Having that in mind, the calculations were performed for two heights of the SE: h =0.5 mm and h = 1 mm. It was found that the smallest variation of the sensitivity is observed when dimensions of the SE are $h \times w \times l = 0.5 \times 2 \times 1$ mm^3 and resistivity $\rho = 80$ Ω·cm. The dielectric constant of the concentrator should be chosen 11.9. The resistance of such a sensor is equal to 800 Ω and sensitivity variation is $\Delta\zeta/\zeta = \pm 9.4$ % within WRD250 waveguide frequency band. It is worth to mention that even smaller sensitivity variation can be found (Fig. 8a), however the resistance of the SE is larger than 1 kΩ

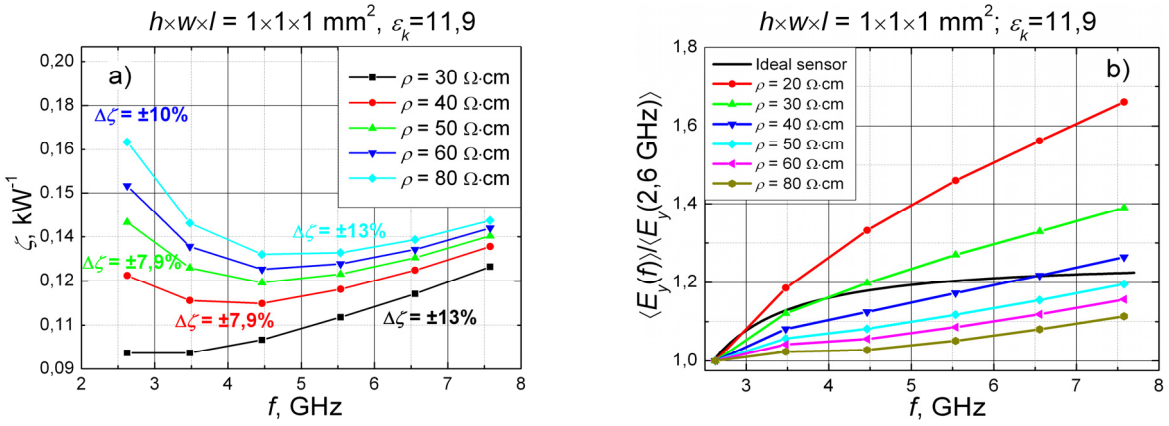

Fig. 8 Calculated sensitivity (a) and relative electric field (b) dependences on frequency for different specific resistance of the SE. The dimensions of the SE are $h \times w \times l = 1 \times 1 \times 1$ mm^3, $\varepsilon_k = 11.9$.

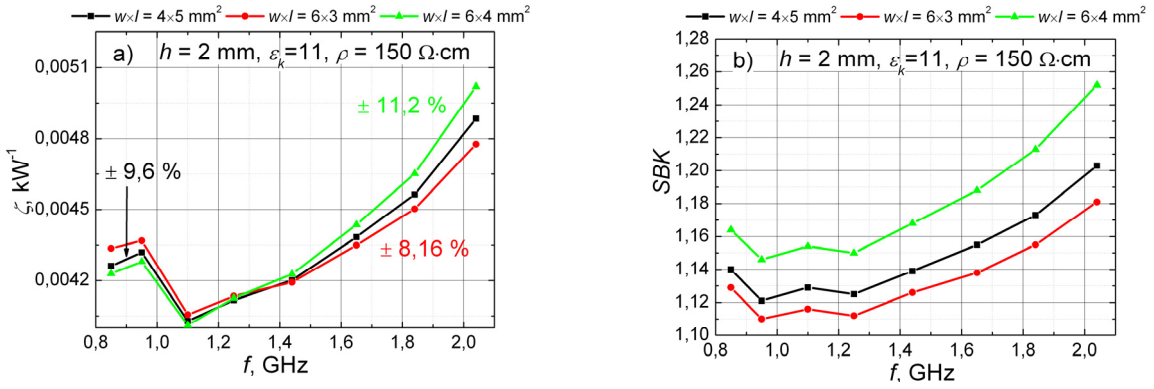

Fig. 9 Calculated sensitivity (a) and VSWR (b) dependences on frequency for the RS implemented in WRD840 waveguide. Resistivity of the SE is $\rho = 150$ Ω·cm, $\varepsilon_k = 11.9$.

3.2.4 Resistive sensor with concentrator (WRD840)

To perform the complete electromagnetic compatibility test of the electronic equipment the sensors capable to measure microwave power from 1 GHz to 10 GHz are required. Therefore after accomplishing simulations of the RS implemented in the WRD250 waveguide we started consideration of the RS with sensing element mounted in the WRD840 waveguide. The pass band of such waveguide is from 0.84 GHz to 2.0 GHz.

The layout of the RS considered is the same as in the previous subsection (ref to Fig. 7). The distance between metal ridges in the WRD840 waveguide is approximately 40 mm. Therefore the first set of calculations was performed to find the optimal height of the SE. It was found that the optimal height of the SE is $h = 2$ mm.

Further simulations were performed for $h = 2$ mm by varying width $w = 2 – 8$ mm, length $l = 2 – 6$ mm and resistivity of the SE. It was found that the smallest sensitivity variation within considered frequency range is characteristic of the SE, the resistivity of which is $\rho = 150$ Ω·cm.·Calculated sensitivity and voltage standing wave ratio dependences on frequency for several cross sectional dimensions of the SE are shown in Fig. 9. It can be seen from Fig. 9a, that the smallest sensitivity variation on frequency demonstrates the SE with the cross-sectional dimensions $w \times l = 6 \times 3$ mm^2. The sensitivity variation of such sensor is $\Delta\zeta/\zeta = \pm 8.2$ % and VSRW < 1.2 (ref to Fig. 9b) within waveguide WRD840 frequency band.

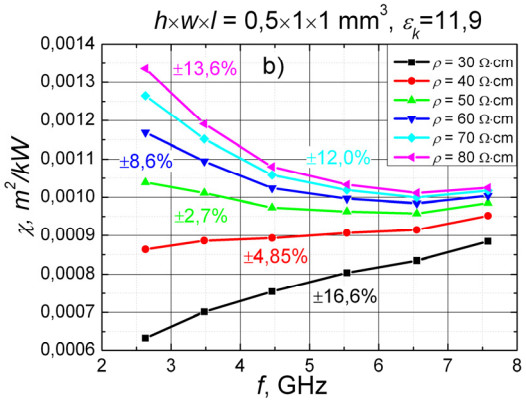

Fig. 10 Dependence of the sensitivity of the system for electric field measurement in free space on frequency for different resistivity sensing elements in WRD250 waveguide: $h \times w \times l = 0.5 \times 1 \times 1$ mm^3, $\varepsilon_k = 11.9$.

3.2.5 Resistive sensors connected to the horn antenna

When performing electromagnetic susceptibility tests the microwave pulse power density (electric field strength) has to be measured. To do that the RS should be connected to the horn antenna. Sensitivity of such measurement system can be written down as follows:

$$\chi = \zeta \cdot S_{eff}, \qquad (2)$$

where S_{eff} is an effective area of the horn antenna.

The effective area of the horn antenna, in turn, depends on gain of the antenna and wavelength of the electromagnetic wave. Therefore, accounting for the dependence of the antenna gain on frequency, when choosing the dimensions and specific resistance of the SE, the system for electric field measurement in free space can be designed, the sensitivity of which is independent of frequency.

In the thesis we demonstrated such approach for a wide band horn antenna ATH2G8 from “Amplifier research”. Simulation results for the RS with concentrator implemented in WRD250 waveguide are shown in Fig. 10. It is seen that by choosing suitable dimensions ($h \times w \times l = 0.5 \times 1 \times 1$ mm^3) and resistivity ($\rho = 50$ Ω·cm) of the SE, the sensitivity variation within ±2.7% in the frequency band of the WRD250 waveguide can be achieved. It is very promising result for the system of the electric field measurement in free space in a wide frequency range.

4 Measurement techniques

In this chapter the measurement techniques and sensors fabrication are described. In the first four sections the measurement setups used in the thesis are presented. In the last section the fabrication of the resistive sensors is described.

4.1 Frequency response measurement

To measure the frequency response of the RS the measurement setup shown in the Fig. 11 was used. It is seen that a low power tunable microwave generator producing roughly 200 mW average power was used. Employing meander modulated microwave signal, the significant increase of the measurement sensitivity was achieved. Actually, two setups with different cross-sectional sizes of the rectangular waveguide windows were used in the experiments. Waveguide WR284 ($a \times b = 73 \times 34$ mm^2) was used in the case of the S band, and waveguide WR159 ($a \times b = 40 \times 20$ mm^2) was employed for the experiments in the C band. The resistive sensor was connected to the main waveguide via transitions from the rectangular to the double ridged waveguide. The tunable microwave source was connected to the rectangular waveguide with the help of a coaxial to rectangular waveguide adaptor. The microwave power supplied to the RS was measured using an average power sensor from Rhode & Schwarz and the output signal from the RS was measured using a lock-in amplifier. The modulation frequency of a microwave signal has been chosen high enough (10 kHz) to avoid additional resistance

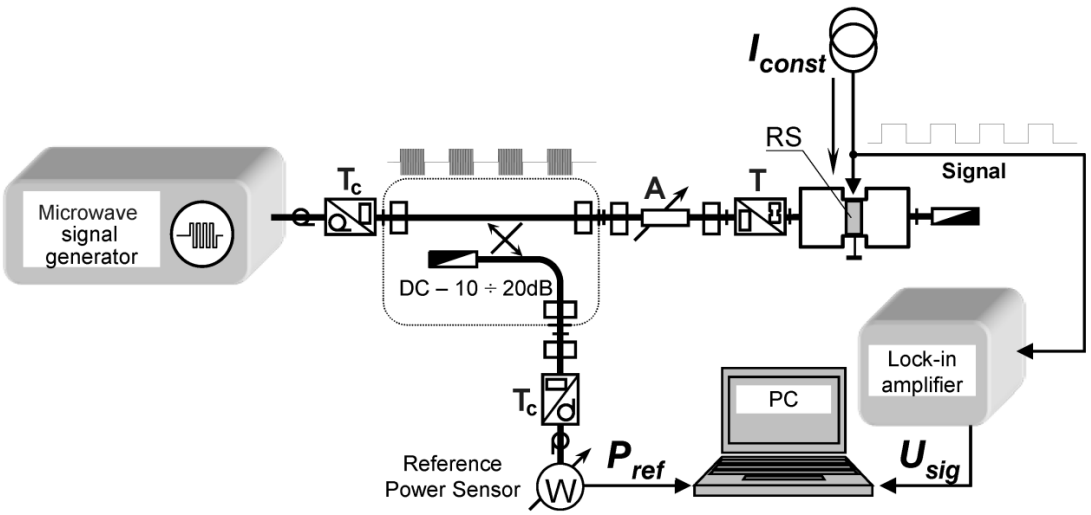

Fig. 11 Measurement set-up using low power tunable microwave source producing roughly 200 mW average power: A – precise attenuator, T – transition from the rectangular to the double ridge waveguide, W – reference power sensor, and RS sensor under test.

modulation due to lattice heating. In this case the sensitivity of the RS can be related with an output signal U_m measured with a lock-in amplifier in the following way:

$$\zeta = \frac{\pi U_m}{\sqrt{2} U_0 P}, \tag{3}$$

where U_0 is a DC voltage drop on the SE.

Thus, by measuring the output signal and power transmitted to the RS, the dependence of the sensitivity on frequency was determined.

4.2 RS output signal measurement

Measurements of the dependence of the RS output signal on pulse power propagating in the waveguide were performed using magnetron generators in S (2.75 GHz) and C (5.7 GHz) frequency bands. The measurement set-up, in general, was similar to that shown in the Fig. 11. Instead of the tunable microwave source the magnetron generator was used to generate high power microwave pulses. The RS was connected directly to the magnetron generator via transition from the rectangular to the double ridged waveguide. Pulse duration was 4 μs and repetition rate was 25 Hz. The reference RS implemented in a rectangular waveguide was connected to the main port via a directional coupler. It controls pulse power in the main waveguide. By changing pulse power in the main port with the help of a precise attenuator, the dependence of the output signal on the pulse power was measured using the oscilloscope TDS520A. The RS was fed by a current source keeping $U_0 = 10$ V. The measurements have been performed with and without an additional amplifier, the amplification of which was $K = 10$.

It is well known [1] that in a wide range of the microwave pulse power, the dependence of $\Delta R/R$ on P can be approximated by the second order polynomial in the following way:

$$P = A\frac{\Delta R}{R} + B\left(\frac{\Delta R}{R}\right)^2, \tag{4}$$

where the coefficients A and B are determined by fitting the experimentally measured dependence of $\Delta R/R$ on P with (2). In the linear region, $\Delta R/R << 1$ and the influence of the second term in (2) is negligible. Therefore the sensitivity of the RS:

$$\zeta = \frac{1}{A} = \frac{U_s}{PU_0}. \quad (5)$$

where U_s is a signal from the resistive sensor under test.

4.3 Measurement of frequency response in WR90 waveguide

A tunable microwave pulse generator HP 8673C was used to generate the sequence of rectangular $\tau = 5$ μs duration and $f = 12.5$ Hz repetition rate microwave pulses. Pulses were amplified by a TWT amplifier up to 100 W and directed to the waveguide switch. The RS under test was connected to the one arm of the waveguide switch while the reference resistive sensor was attached to the other one. By toggling the position of the switch from the one arm to the other, the output signals from the RS under test and the reference sensor were measured. Signals from both devices were observed on the screen of the oscilloscope. As in a previous case, the RS was fed by a current source keeping 10 V voltage drop on the SE. The sensitivity of the resistive sensor was calculated using (5).

4.4 Measurements in free space

Experimental investigations of the resistive sensor connected to the horn antenna were performed in the semi-anechoic chamber of microwave laboratory. The measurement setup is shown in Fig. 12. The duration of microwave pulses used in experiments was 10 μs, their repetition rate was 100 Hz. Maximum microwave pulse power used in experiments was 2 kW. As one can see from the figure, the microwave power passed to the transmitting antenna was controlled by the reference resistive sensor. At the distance l from the transmitting antenna the receiving antenna connected

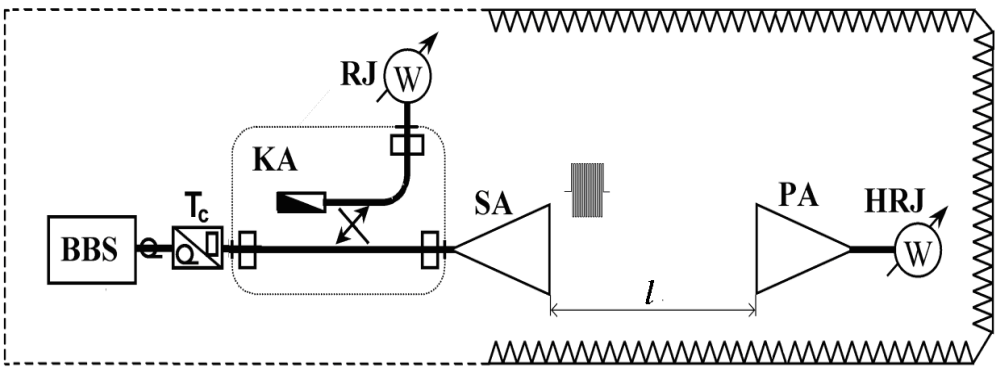

Fig. 12 Experimental set-up for investigation of the resistive sensor connected to the horn antenna: HRJ – resistive sensor under test, SA and PA – transmitting and receiving horn antennas, respectively RJ – resistive sensors measuring microwave pulse power conveyed to the transmitting antenna.

to the resistive sensor was placed. Sensitivity of the measurement system composed of the wide band horn antenna and the resistive sensor under test can be written as:

$$\chi = \frac{4\pi l^2 U_s}{U_0 G_s P} \tag{6}$$

where U_s is the signal measured from the RS connected to receiving antenna, P and G_s are a power conveyed to the transmitting antenna and its gain, respectively.

4.5 Fabrication of resistive sensors

The sections of corresponding waveguides and sensing elements should be manufactured before the resistive sensor could be assembled. To manufacture the SE the slice from a monocrystal of n-type Si was cut, the thickness of which after polishing should correspond to the height h of the SE. Following wafer preparation, the diffusion of phosphorus impurities from both sides of the wafer was performed. After diffusion, Al-V-Cu metal contacts were evaporated forming ohmic contacts on both sides of the wafer. Finally, to provide good quality electrical contact with waveguide section, the Au layer was electrochemically deposited on the wafer. After contact formation wafer was cut into suitable length and width samples which are mounted in the waveguide sections.

5 Measurement results

In this chapter measurement results are described. In the first two sections measurement results of the resistive sensors implemented in WR90 and WRD250 waveguides are presented. The last section is devoted to the electric field measurements in free space using the resistive sensor connected to the wide band horn antenna.

5.1 WR90 resistive sensor

In this section experimental investigation of the frequency response and sensitivity of the resistive sensor implemented in the WR90 is reviewed. Operating frequency of the WR90 waveguide is from 8.0 GHz to 12.4 GHz.

Initially, sensor's output signal dependence on microwave pulse power was measured using magnetron generator at f = 9.4 GHz. Measurement setup is described in section 4.2. Afterwards the dependence of the sensitivity on frequency was determined

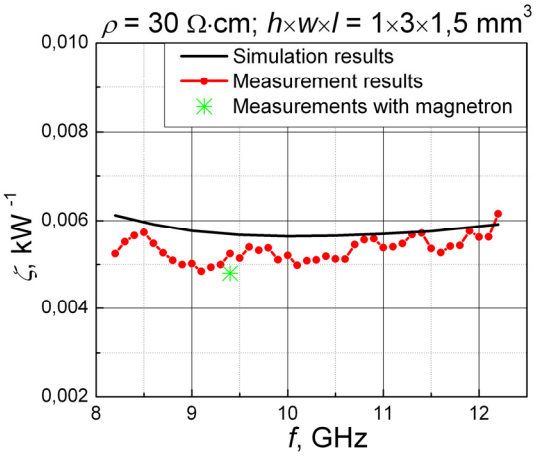

Fig. 13 Frequency response of WR90 resistive sensor. Line shows simulation results, points demonstrate measurement results, and star indicates measurements with high power microwave pulses.

employing setup described in section 4.3. Measurement results are shown by points in Fig. 13. In the figure the sensitivity value calculated from the experiments performed with magnetron generator is also shown by a star. Comparing measured results with calculated (Fig. 13), one can see that the reasonable agreement between calculated and measured values of ζ has been obtained. Measured sensitivity variation of the resistive sensor in the frequency band of the WR90 waveguide was ±9.1%.

It should be pointed out that the sensitivity of the designed and manufactured sensor is sufficiently lower than the analogous sensors, the SE of which is placed under metal diaphragm [6]. However, the sensor's output signal dependence on power is much more linear in a high power region; consequently, it could found application for the measurement of very high microwave power pulses in a rectangular waveguide.

5.2 WRD250 resistive sensors

In this section the experimental results of the cross waveguide type WRD250 resistive sensor is presented. Two types of the resistive sensors were manufactured in accordance with the modelling results presented in the subsection 3.2.2. The dimensions and specific resistance of the manufactured sensors were the following: $h\times w\times l = 3.8\times1\times1$ mm^3, $\rho = 10$ Ω·cm and $h\times w\times l = 3.8\times1\times2$ mm^3, $\rho = 50$ Ω·cm.

Initially, sensors' output signal dependences on microwave pulse power were measured at 2.75 GHz and 5.7 GHz using measurement setup presented in the section 4.2. The output characteristic of the sensors was measured up to a twofold increase of their resistance. It was found that measured dependence fits well polynomial

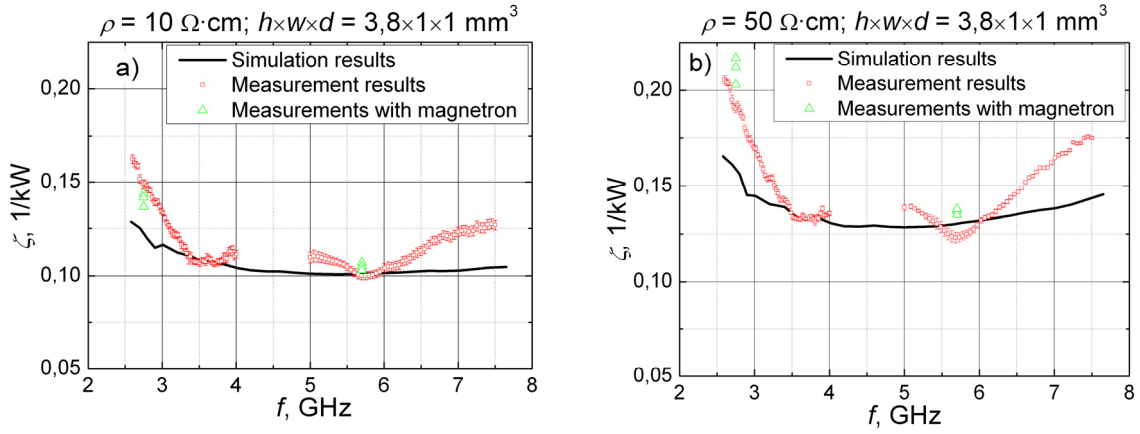

Fig. 14 Frequency response of the RS implemented in WRD250 waveguide. SE parameters: (a) $\rho = 10$ Ω·cm, $h \times w \times l = 3.8 \times 1 \times 1$ mm^3, (b) $\rho = 50$ Ω·cm, $h \times w \times l = 3.8 \times 1 \times 2$ mm^3. Points with error bars show averaged measurement results, triangles show measurement results using magnetron generators, line demonstrate simulation results.

approximation (4). From the value of the coefficient A, the sensitivities of the RS in the linear region were determined. It was found that at a lower frequency sensors are more sensitive than at a higher one. Experimental investigations have revealed that the RS implemented in the double ridged waveguide is able to measure pulse power from a few watts up to a few tens of kW.

The results of the measured frequency response of the RS together with calculation results are shown in Fig. 14. Three different samples of the RS have been measured using the meander modulated microwave signal and lock-in amplifier technique described earlier in section 4.1. As follows from the figure, the sensitivities determined from experiments with magnetron generators (triangles) fit well the results obtained using the meander modulated technique. By comparing the measured results with calculated one using the FDTD method one can see that a reasonable agreement between them was obtained. In comparison with the theoretical prediction, the measured results demonstrate a larger variation of sensitivity that is roughly ±24%. Although the measured variation of the sensitivity of the RS implemented in the double ridged waveguide is larger than expected, their good reproducibility and increased frequency range are promising features for the application of the proposed sensors in HPM experiments.

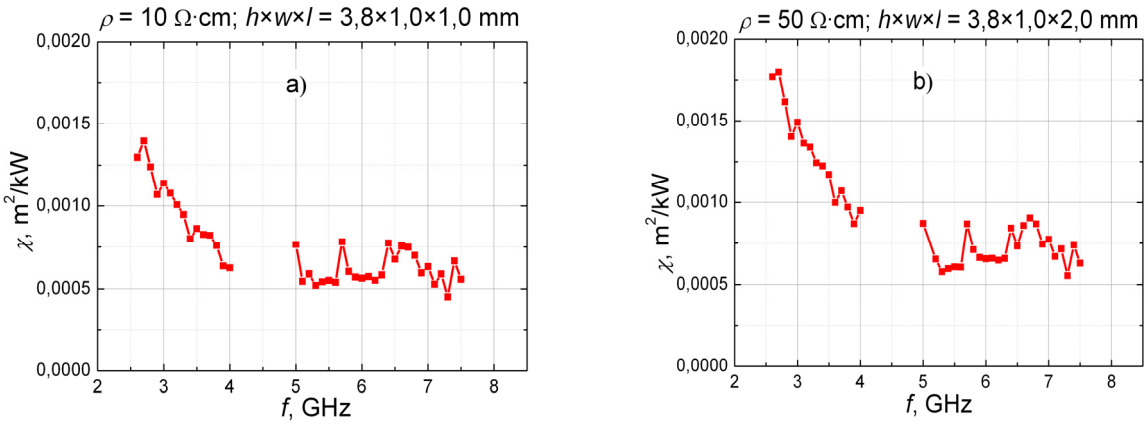

Fig. 15 Frequency response of the resistive sensor connected to the horn antenna. SE parameters: (a) $\rho = 10$ Ω·cm, $h \times w \times l = 3.8 \times 1 \times 1$ mm^3, (b) $\rho = 50$ Ω·cm, $h \times w \times l = 3.8 \times 1 \times 2$ mm^3.

5.3 Measurements in free space

In this section measurement results of the resistive sensors connected to the horn antenna is described. Calibrated wideband horn antenna LB-2678-10-C-NF produced by A-INFOMW (China) was used in the measurements. The purchased horn antenna was compatible with WRD250 waveguide, so it was connected to the developed RS comprising the measurement system suitable for microwave pulse power density measurements in free space. Measurement setup is presented in section 4.4. For transmitting of microwave pulses into semi-anechoic chamber we used calibrated S and C band horn antennas connected to the rectangular waveguides.

Measured dependences of the sensitivity of the measurement system on frequency for two different sensors are shown in Fig. 15. It is seen that in both cases sensitivity strongly decreases in the frequency range 2.6 – 4 GHz and becomes practically independent of frequency in 5 – 7.5 GHz band. One can conclude that in this frequency range resistive sensor's sensitivity response is compensated by the antenna gain frequency response leading to the measurement system, the sensitivity of which is independent of frequency. This result in fact, confirms our suggestion made in subsection 3.2.5 that accounting for the dependence of the antenna gain on frequency, when choosing dimensions and specific resistance of the SE, the system for electric field measurement in free space can be designed, the sensitivity of which is independent of frequency.

6 Electromagnetic susceptibility tests

In this chapter electromagnetic susceptibility test results of internet routers and media converters are presented. In the tests the RS connected to the horn antenna was used for the measurement of the electric field strength near the device under the test demonstrating possible practical application of the resistive sensor. In the first two sections the thermal heating and parasitic charging models are presented and expressions binding threshold electric field with HPM pulse duration and repetition rate are derived. Experimental setup and susceptibility levels are described in the third section. The last two sections of the chapter are devoted to the description of experimental results.

6.1 Thermal heating model

In a microwave region electromagnetic field affecting the device under the test is characterized by the radiated electric field amplitude E. Let us assume that the sequence of microwave pulses, duration of which is τ and repetition period T, is applied to the device under the test and the overheating of some region of the device is responsible for the failure of the device. Considering the energy balance equation describing the overheating of the device, one can express the amplitude of the threshold electric field causing the failure of the electronic device, as follows:

$$E_{th} = \sqrt{\frac{Z_0 cdl\Delta T_{max}}{\tau_h(1-\exp(-\tau/\tau_h))}}, \tag{7}$$

where Z_0 is an impedance of free space, c is a specific heat capacity, d is a density, l is a length of region, where the power is absorbed, and $\Delta T_{\max}$ is an increase of temperature, at which failure of the device occurs. It should be pointed out that (7) has been written down assuming that $T >> \tau_h$, where τ_h is a characteristic thermal relaxation time.

6.2 Parasitic charging model

Considering the failure of the device one can suppose that the external electric field induces some parasitic voltage in the circuitry of the device $U=El$ where l is the length of the circuit that serves as an antenna. The induced voltage through the p-n junction can charge the capacitor in the circuit up to voltage U_m, at which the failure of the device

occurs. Let charging and discharging times be denoted as τ_c and τ_d, respectively. Assuming that $\tau << \tau_d$ and, considering equation very similar to that in the previous section, one can get the following expression describing the threshold electric field, which causes the failure of the device due to parasitic charging:

$$E_{th} = \frac{\pi U_m}{l} \frac{1 - exp\left(\frac{\tau}{\tau_d} - \frac{T}{\tau_d} - \frac{\tau}{\tau_c}\right)}{1 - exp\left(-\frac{\tau}{\tau_c}\right)}, \quad (8)$$

As follows from (7) and (8) the threshold electric field depends on pulse duration and repetition period. If such dependence is found experimentally by fitting experimental results with (7) or (8), one can ensure whether thermal heating or parasitic charging is responsible for the failure of the device.

6.3 Electromagnetic susceptibility tests

Electromagnetic susceptibility tests were performed in a semi-anechoic chamber. Experimental setup was similar to that previously described in section 4.4 (Fig. 12) except for the fact the electronic devise under the test was placed near the receiving horn antenna. To generate HPM pulsed S (2.75 GHz), C (5.7 GHz) and X (9.3 GHz) band magnetrons were used. The strength of the HPM electric field E was measured with the resistive sensor connected to the receiving horn antenna. The pulse power conveyed to the transmitting antenna was measured by the other RS connected to the main port via directional coupler. The test object and receiving antenna were located in a far zone of antennas. Since the gain of both antennas is known, on the one hand, the electric field in the test point can be determined from the power P measured with the reference sensor:

$$E_s = \frac{1}{l}\sqrt{\frac{2Z_0 G_s P}{4\pi}}, \quad (9)$$

where G_s is a gain of the transmitting horn antenna, l is the distance between the transmitting antenna and the device under the test, and Z_0 is an impedance of free space. On the other hand the electric field strength can be found from the measured pulse power P_p with the RS connected to the receiving antenna:

$$E_p = \sqrt{\frac{8\pi Z_0 P_p}{G_p \lambda^2}}, \tag{10}$$

where G_p is a gain of the receiving horn antenna and λ is the wavelength of electromagnetic wave in free space.

Several levels are used to characterize the degradation of communication performance of the device affected by HPM pulses. Considering *PING* packet and *FTP* protocol as a tools used to determine the influence of HPM radiation on network communication performance the following levels have been set:

L0 – "weak effect". Below L0 no effect is observed, at L0 the speed of data transfer via *FTP* protocol starts to decrease, but *PING* packets are not lost yet.

L1 – "medium interference". The lost *PING* packets are observed.

L2 – "strong interference". Data traffic is entirely blocked, but performance is self-recovered, when HPM radiation is switched off.

L3 – "upset". The performance is not self-recovered, when radiation is switched off, the device stays in "upset" state, until operator restarts the device.

L4 – "damage". Physical damage of device, the replacement of elements is needed.

6.4 Susceptibility of internet routers

Three internet routers: wireless 100/1000 Mb/s speed router, and two wired 10/100 Mbs and 100/1000 Mb/s speed routers were tested for susceptibility level L3 ("upset"). Two main investigations were done: (i) dependence of the threshold electric field E_{th} for level L3 on microwave frequency and wave polarisation, and (ii) dependence of E_{th} on HPM pulse duration and repetition rate. The dependence of E_{th} on frequency in normalized units is shown in Fig. 16. The experiments were carried out at HPM pulse duration 1 μs, and repetition rate 12.5 Hz. As it is seen from the figure, the threshold electric field strongly depends on frequency and direction of radiation.

The susceptibility of older generation (10/100 Mb/s) device, in general, decreases with frequency, but 1 Gb/s router is the most susceptible at C band (5.7 GHz). The susceptibility of this device in C band is even larger than for wireless one in S band. It can be explained by faster circuitry elements, which becomes more susceptible at higher frequency due to their smaller dimensions. It might be expected that the further decrease

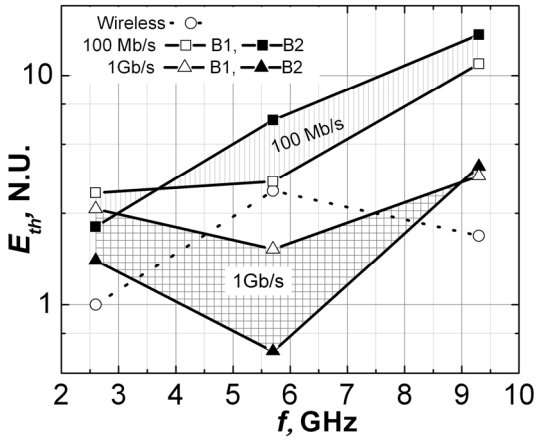

Fig. 16 Dependence of the threshold electric field E_{th} of the internet routers on frequency for susceptibility level L3 (upset). Electric field strength is shown in normalized units. The filled area demonstrates the range of L3 in two different polarizations of the HPM electric field.

of circuitry element size, when communication speed increases, results in more susceptible future devices at higher frequency.

Some dependences of E_{th} on pulse duration and repetition rate were found for older generation router and 1 Gb/s device. Within available HPM pulse duration both thermal heating and parasitic charging models considered in the previous sections fit well experimentally measured data. To distinguish which model is more suitable, the experiments with shorter pulses of the order of 100 ns or even shorter should be performed.

6.5 Susceptibility of media converters

Six models of media converters were tested to reach the susceptibility levels L0-L4 at the same frequencies as the tests on routers. Tests were done using different HPM pulse durations and repetition rates but the dependence of E_{th} neither on pulse duration, nor on repetition rate has been observed. Possibly, the time constants of modern media converters are considerably shorter than the duration of HPM pulses used in the tests.

It was found that media converter “MOXA” in plastic enclosure is the only device that do not reach level L3 within considered frequency and electric field strength range. All other five models of tested devices reached level L3, and one of them was even damaged (L4). It is worth to mention that except “MOXA” all other tested devices are placed in metallic boxes and this might be the reason of a larger susceptibility observed experimentally. One can assume that the metallic enclosure can act as a resonator cavity at some frequency, resulting in strong increase of the susceptibility level.

7 Results and conclusions

- Using finite-difference time-domain method the optimal parameters of the sensing elements mounted in WR90, WRD250 and WRD840 waveguides were determined.
- Using finite-difference time-domain method for the modelling of the resistive sensors, it was noticed that by changing transverse dimensions or specific resistance of the sensing element, the character of the dependence of the relative electric field strength inside the sensing element on frequency can be changed. This, in turn, has allowed us to optimize the frequency response of the resistive sensor.
- Accounting for the horn antenna characteristics when choosing the parameters of the sensing element, allows us to develop a measurement unit, consisting of the horn antenna and resistive sensor, for measuring microwave pulse power density (electric field strength) in free space with flat frequency response.
- Sensitivity variation ±9.1% and ±25% has been found experimentally for resistive sensors implemented in WR90 and WRD250 waveguides, respectively, in the pass band of the corresponding waveguide.
- Designed and manufactured resistive sensors implemented in WRD250 waveguide measure microwave pulses from a few watts, and their dynamic range is 50 dB.
- The dependence of the threshold electric field for the upset level (L3) on frequency, pulse duration and repetition rate has been determined for three different type internet routers. It was found that older generation 100 Mb/s speed router is less susceptible to HPM radiation in comparison with wireless and 1 Gb/s routers.
- Observed dependence of the threshold electric field for upset level (L3) on pulse duration and repetition rate for internet routers can be clarified neither by thermal heating nor by parasitic charging models. In order to prove one

of the considered models, the measurements with shorter then $\tau = 0.7$ μs high power microwave pulses is desirable.

- Experimental investigations of the susceptibility of the media converters strongly confirms the assumption that metallic enclosure can act as a resonator cavity at some frequency, resulting in a strong increase of susceptibility level of the device.

References

[1] M. Dagys, Ž. Kancleris, R. Simniškis, E. Schamiloglu, and F. J. Agee, "The resistive sensor: a device for high-power microwave pulsed measurements," *Antennas and Propagation Magazine, IEEE,* vol. 43, pp. 64-79, 2001.

[2] S. B. Cohn, "Properties of ridge waveguide," *Proceedings of the IRE,* vol. vol. 35, pp. 783-788, August 1947.

[3] S. Hopfer, "The design of ridged waveguides," *Microwave Theory and Techniques, IRE Transactions on,* vol. 3, pp. 20-29, 1955.

[4] D. Wunsch and R. Bell, "Determination of threshold failure levels of semiconductor diodes and transistors due to pulse voltages," *Nuclear Science, IEEE Transactions on,* vol. 15, pp. 244-259, 1968.

[5] A. Taflove and S. C. Hagness, *Computational electrodynamics* vol. 160: Artech house BostonLondon, 2000.

[6] Ž. Kancleris, R. Simniškis, M. Dagys, V. Tamošiūnas, and P. Ragulis, "Experimental Investigation of High Pulse Power Microwave Resistive Sensor with Flat Frequency Response," *ACTA PHYSICA POLONICA A,* vol. 115, 2009.

[7] Ž. Kancleris, R. Simniškis, M. Dagys, and V. Tamošiūnas, "X-band resistive sensor for high-power microwave pulse measurement with flat frequency response," *Electronics Letters,* vol. 44, pp. 1143-1144, 2008.

List of articles related to the thesis:

Referred in Web of Science:

- Ž. Kancleris, P. Ragulis, R. Simniškis, and M. Dagys, "Wide band waveguide sensor for microwave pulse measurement" Lithuanian Journal of Physics Vol. **53**, No. 2, pp. 99–103 (2013)
- Ž. Kancleris and P. Ragulis. "Interaction of semiconductor sample with TE10 mode in double ridged waveguide." Lithuanian Journal of Physics Vol. **52,** No. 1, pp. 1–9 (2012).
- M. Dagys, Ž. Kancleris, P. Ragulis, R. Simniškis, and V. Tamošiūnas, "Investigation of susceptibility of routers to high power microwave pulse radiation," in Microwave Radar and Wireless Communications (MIKON), 2010 18th International Conference, Vol. 1 pp. 126-128 (2010).
- P. Ragulis, V. Tamošiūnas, Ž. Kancleris, R. Simniškis, and M. Tamošiūnienė, "Optimisation of resistive sensor for ridge waveguide," in Microwave Radar and Wireless Communications (MIKON), 2010 18th International Conference, Vol. 2 pp. 714-717 (2010).
- Ž. Kancleris, R. Simniškis, M. Dagys, V. Tamošiūnas, and P. Ragulis, "Experimental Investigation of High Pulse Power Microwave Resistive Sensor with Flat Frequency Response," Acta Physica Polonica A, vol. Vol. 115, No. 6, pp. 1122-1124 (2009)

List of articles in other publications:

- Ž. Kancleris, R. Simniškis, P. Ragulis, M. Dagys, Investigation of susceptibility of network switches and media converters to high power microwave pulse radiation, NATO RTO SCI-232; Norfolk, USA, May 10-11, 2011.

Presentations in scientific conferences:

- Ž. Kancleris, P. Ragulis, R. Simniškis, M. Dagys, „Susceptibility of computer network components to high power microwaves", EUROEM 2012, 2-6 July 2012, Toulouse France.

- Ž. Kancleris, P. Ragulis, R. Simniškis, M. Dagys, „Resistive sensor for high power microwave pulse measurement in double ridged waveguide“ , EUROEM 2012, 2-6 July 2012, Toulouse France.
- P. Ragulis, Ž. Kancleris, G. Šlekas, R. Simniškis, M. Dagys, “Skersai bangolaidžio įtvertas rezistorinis jutiklis H tipo bangolaidžiui”, 39-oji LNFK, 2011 spalio 6-8 d., Vilnius.
- M. Dagys, Ž. Kancleris, P. Ragulis, R. Simniškis, “Resistive sensor for high power microwave pulse measurement”, ICEAA'11; Torino, Italy, September 12-16, 2011.
- P. Ragulis, Ž. Kancleris, R. Simniškis, “Impact of high power microwave radiation on functionality of switches and media converters”, Electronics'2011, Kaunas and Vilnius, May 17-18,
- M. Dagys, Ž. Kancleris, P. Ragulis , R. Simniškis, V. Tamošiūnas, „Investigation of susceptibility of routers to high power microwave pulse radiation“, Microwave Radar and Wireless Communications (MIKON), 2010 18th International Conference.
- P. Ragulis, V. Tamošiūnas, Ž. Kancleris, R. Simniškis, M. Tamošiūnienė, „Optimisation of resistive sensor for ridge waveguide”, Microwave Radar and Wireless Communications (MIKON), 2010 18th International Conference.
- P. Ragulis, V. Tamošiūnas, Ž. Kancleris, R. Simniškis, M. Tamošiūnienė, „Optimisation of Resistive Sensors for H Type Microwave Waveguides“, E2010 14th International Conference On Electronics.
- V. Tamošiūnas, Ž. Kancleris, R. Simniškis, P. Ragulis, M. Tamošiūnienė, „Rezistorinių mikrobangų jutiklių optimizavimas H tipo bangolaidžiams“, („Optimisation of resistive sensors for H type microwave waveguides“), 38-oji Lietuvos nacionalinė fizikos konferencija.

About the author

Name and surname:	Paulius Ragulis
Birth date and place:	April 25, 1984, Šiauliai, Lithuania
E-mail:	rpaulius@pfi.lt

Education:	2006	Bachelor Degree in Physics, Vilnius University
	2008	Master Degree in Physics, Vilnius University
	2008-2012	PhD studies, Center for Physical Sciences and Technology and Vilnius University
Scientific experience:	2004 – 2007	Technician, Semiconductor Physics Institute
	2007 – 2008	Engineer, Semiconductor Physics Institute
	2008 – 2010	Junior scientific researcher, Semiconductor Physics Institute
	2010 – 2013	Junior scientific researcher, „Modernios E-Technologijos“
	2011 – till now	Junior scientific researcher, Center for Physical Sciences and Technology, Semiconductor Physics Institute

Publications: co-author of 7 articles and 17 presentations in the conferences.

Scientific projects: participant of 6 national and international projects.